POLISH MARITIME RESEARCH 4 (124) 2024 Vol. 31; pp. 76-88
10.2478/pomr-2024-0052

Thermodynamic Efficiency of an Advanced 4th Generation VHTR Propulsion Engine for Large Container Ships

Jerzy Głuch [1]
Tomasz Kodlewicz [1]
Marta Drosińska–Komor [1]*
Natalia Ziółkowska [2]
Łukasz Breńkacz [3]
Paweł Ziółkowski [1]

[1] Gdańsk University of Technology, Faculty of Mechanical Engineering and Ship Technology, Poland
[2] Gdańsk University of Technology, Doctoral School, Poland
[3] Institute of Fluid Flow Machinery, Polish Academy of Sciences, Gdańsk, Poland

* Corresponding author: *marta.drosinska@pg.edu.pl (M. Drosińska-Komor)*

ABSTRACT

In response to global initiatives to reduce greenhouse gas emissions, the maritime industry must adopt green propulsion solutions. This paper analyses the operational potential of very high-temperature reactors (VHTRs) as an innovative propulsion source for large container ships. Calculations are carried out for ships produced between 2018 and 2020 with a capacity of more than 20,000 TEU. For these ships, the average power of the main system is calculated at around 64.00 kW. The study focuses on a propulsion engine system with features such as extraction control, bypass control, and either one or two turbines. The direct thermodynamic cycle of the VHTR offers high efficiency, smaller sizes, and flexible power control, thus eliminating the need for helium storage and enabling rapid power changes. In addition, this article highlights the advantages of bypass control of the turbine, which avoids the need to shut down the propulsion engine in the harbour. The findings suggest that nuclear propulsion could play a crucial role in the future of maritime technology.

Keywords: nuclear propulsion engine, reactor, CO_2 reduction, energy efficiency, sustainable development

NOMENCLATURE

a	– speed of sound [m/s]
A_C	– total flow area of the medium on one side of the regenerative heat exchanger
BV	– bypass valve
C	– compressor
COOL	– cooling system
CO_2	– carbon dioxide
c_p	– specific heat capacity
C_{pHe}	– averaged specific heat capacity of helium, kJ/kg
C_{pw}	– averaged specific heat capacity of water, kJ/kg
T_C	– compressor turbine
d_h	– hydraulic diameter
D_R	– core diameter
EU	– European Union
EU ETS	– European Union Emissions Trading Scheme
f	– friction coefficient
G	– generator
H_R	– core height
i_n	– enthalpy at point n
L	– length of the exchanger
l_C	– unit work of compressor, kJ/kg
l_T	– unit work of the turbine, kJ/kg
$l_t = l_T – l_C$	– unit technical work of cycle, kJ/kg
M	– molar mass of gas, kg/mol

$\dot{m}_{He}$ – mass flow rate for helium, kg/s
$\dot{m}_{TM}$ – mass flow rate in the power turbine
$\dot{m}_{TC}$ – mass intensity in the compressor turbine
$\dot{m}$ – mass flow rate
N_e – effective power of the turbine
$N_{e100\%}$ – effective power at full load
N_{ep} – effective power at partial load
P_a – pressure of the medium at the reactor inlet
N_{TP} – steam turbine power
$\dot{Q}_R$ – thermal power of the reactor
q_R – specific heat dissipated to the working medium in the reactor
R – universal gas constant [J/(molK)]
R – reactor
RE – regenerative heat exchanger
T – absolute temperature [K]
TA – tank
T – turbine
T_C – compressor turbine
T_P – power turbine
TV – tank valve
T_1 – temperature at the inlet to the compressor [K]
T_4 – temperature of the medium at the downstream end of the reactor [K]
t_n – medium temperature at n–point
$t_{w'}$ – water temperature [°C]
$t_{w''}$ – temperature of water at the cooling system outlet [°C]
UN – United Nations
UNFCCC – United Nations Framework Convention on Climate Change
VHTR – very high-temperature reactor
V_R – core volume
δ_{COOL} – efficiency of a cooling system
ΔP – power decrease
Δp – pressure loss
Δp_{COOL} – pressure loss in the heat exchanger of the cooling system
Δp_r – pressure loss in the reactor
Δp_{RE-LP} – pressure loss in the regenerative heat exchanger on the low-pressure side
Δp_{RE-HP} – pressure loss in the regenerative heat exchanger on the high-pressure side
δ_{RE} – regenerative heat exchanger efficiency
ΔT_{RE-LP} – temperature difference on the low-temperature side of the regenerative heat exchanger [K]
$\eta_{100\%}$ – efficiency of the cycle at full load
η_p – efficiency of the cycle at partial load
η_{iC} – compressor efficiency
η_{iT} – turbine efficiency
κ – gas adiabatic exponent
Π_T – turbine expansion ratio
ρ – density
φ_R – core power density

INTRODUCTION

The need to protect the environment, including reducing greenhouse gas emissions, has been discussed worldwide for many years [1]. Currently, the main problems in this regard are the excessive production of greenhouse gases, especially CO_2, NO_X, and SO_X [2,3], and the effects these gases cause [4]. In the Declaration of the United Nations Conference on the Human Environment in 1972, the need to protect the environment was specified [5], and environmental protection continues to be discussed at world congresses. The first World Climate Conference was held in 1979 in Geneva [6,7]. One of the most important documents in this domain is the Paris Agreement, which was signed in 2015 [8,9] and aims to limit the global temperature increase to a maximum of 2°C [10] compared to the temperature prevailing before the industrial era [11]. The European Union has set itself the target of becoming climate neutral by 2050 by implementing the obligations imposed on it [12].

Transport has a very large impact on the production of gases and the associated increase in temperature. Currently, around 70% of all cargo is transported by ship. Greenhouse gas emissions in the European Union amount to 4% of its total CO_2 emissions, representing more than 144 million tons of CO_2 per year. Domestic shipping accounts for 0.4% of total greenhouse gas emissions, while international shipping produces approximately 3.6% [13]. In 2018, the shipping sector was responsible for producing 2.9% (1,076 million tons of CO_2) of the total greenhouse gases released into the atmosphere [14]. Although the amount created by the shipping sector seems small compared to the overall amounts of greenhouse gases produced, this sector is growing the fastest next to aviation. The effects are especially visible if we compare the amount of greenhouse gas emissions generated in 1990 with the current state, as there has been an increase in production of 34%. The European Union has prepared a document called the "Fit for 55" package, the main postulate of which is to reduce greenhouse gas emissions by at least 55% compared to the amount produced in 1990 [15]. One of the assumptions made in this document is that the EU Emissions Trading Scheme (EU ETS) also applies to maritime transport [16]. In view of the various requirements that have been set by world authorities, it is necessary to introduce new technologies to protect the environment. We have the opportunity to prevent catastrophic consequences for the environment and for humanity [17,18]. Since new technologies are increasingly required to be ecologically friendly, and to strive for zero emissions, there are works in the literature that have focused on the possibility of using reactors to power ships in various types of systems, from steam to gas. An example of a steam system with a reactor is presented in [19].

This work describes a combination of a VHTR reactor with a gas turbine installation which can be used to power ships. The ecological and thermodynamic efficiency characteristics are most important to achieve the longest possible service period, i.e. moving at a cruising speed rather than manoeuvring times. The load corresponding to such conditions and the configurations of the full speed power engine are analysed in the section entitled

'Sea water temperature'. We also analyse the thermodynamic capabilities of an engine based on a turbine and reactor cycle, and the results are presented in the section entitled 'Variation in propeller engine power demand'. A breakdown of results from the control analysis of the engine propulsion system and the marine propeller is shown in Fig. 1. This article exclusively addresses the thermodynamic aspect of the cycle of a helium-based gas turbine, and attention is focused on large container ships produced between 2018 and 2020 that have a capacity of more than 20,000 TEU.

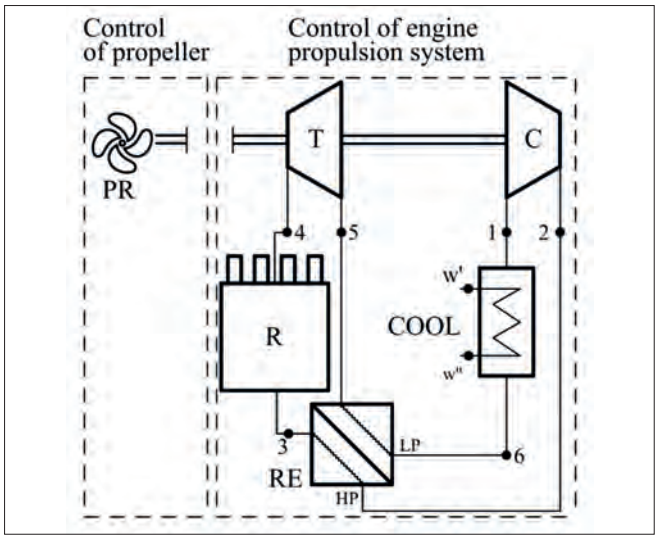

Fig. 1. Closed cycle, where T–turbine, C–compressor, R– VHTR, PR –power receiver, RE – regenerative heat exchanger (LP – low-pressure side, HP – high-pressure side), COOL–cooling system. Characteristic points 1–6

PROPOSED PROPULSION SYSTEM WITH VHTR FOR A CONTAINER SHIP

The main parameter affecting the size of the propulsion solution for a container ship is the power requirement. Several examples of ships built between 2018 and 2020 with a capacity of more than 20,000 TEU were selected for this study, and the data collected on these ships are presented in Table 1. In the selection process used to evaluate these vessels, we made several key assumptions based on production time and performance. Firstly, we concentrated primarily on large ships, especially those with a capacity exceeding 20,000 TEU. Thus, this research focused on large-scale objects, and the technology used to produce them remained relatively constant over time. Secondly, we referred to our previous work [19], which highlighted the potential use of VHTR for ship propulsion and the feasibility of incorporating such reactors into the steam cycle, and provided insights based on sample ships from 2018. The novelty of the present work in comparison to the previous work is the introduction of a new thermodynamic cycle based on a gas turbine and a new perspective medium, i.e. helium.

In this research on VHTR reactors for marine propulsion, we selected ships manufactured between 2018 and 2020. This time frame was chosen to ensure that the analysed vessels were relatively new and used the latest advances in marine technology, making our research relevant.

The dimensions and contract speeds of the chosen ships were similar to each other. It was decided to calculate the arithmetic average power of the main engines in order to select a representative case for further calculations. The calculated average power was 63.580 kW, which was rounded to 64 kW for the subsequent calculations.

Tab. 1. Summary of selected container ships built between 2018 and 2020 and with a capacity of more than 20,000 TEU [20–22]

	CMA CGM Jacques Saade	HMM Algeciras	HMM Oslo	MSC Gülsün	CMA CGM Antoine De Saint Exupery
Length [m]	399.9	399.9	399.9	399.9	400
Width [m]	61.3	61	61.5	61.5	59
Immersion [m]	16	16.5	16.5	16.5	16
Deadweight [DWT]	221,250	232,700	228,600	228,600	202,600
Cargo capacity [TEU]	23,112	23,964	23,820	23,756	20,600
Power of main engine [kW]	63,840	60,380	59,600	66,650	67,430
Contract speed [kn]	22	22.4	22.25	22	21.5
Year of manufacture	2020	2020	2020	2019	2018

To ensure the safety of the ship's crew and the environment, the use of a VHTR reactor to power ships is suggested [23]. The proposed reactor uses helium as a coolant, which effectively removes heat from the reactor core even at temperatures of up to 1000°C. As a noble gas, helium is chemically inert, which means that it does not react with the materials used to construct the reactor or nuclear fuel, thereby minimising the risk of explosions or dangerous chemical reactions. Helium also has high thermal stability and remains in a gaseous state over a wide range of temperatures and pressures, making it a reliable coolant in emergencies. HTGR reactors such as VHTR use passive safety systems, which allow the helium to continue to dissipate heat even without active cooling, and this can be crucial in preventing the core from overheating. An additional form of security in this system is the use of fuel in the form of TRISO balls, each of which has protective coatings that allow it to operate at very high temperatures of up to 1600°C. In other words TRISO stands for TRi-structural ISOtropic particle fuel. The multilayer design of TRISO balls effectively prevents the release of radioactive substances during the fission process [24], an extremely important aspect when the reactor is installed on a ship. The use of TRISO fuel also allows for long-term operation without the need for frequent replacement [25], which is especially important during long cruises far from land. In summary, the use of helium and TRISO fuel in VHTR reactors significantly increases the safety

of a reactor for use on ships, protecting both the environment and people on and near ships.

SELECTION OF A CONTROL METHOD FOR THE THERMODYNAMIC CYCLE OF THE PROPULSION SYSTEM

Two types of turbines can be used in propulsion systems, based on steam or gas [26,27]. A gas propulsion solution can operate using an indirect or direct cycle [28]. With a direct cycle, a higher efficiency is obtained than with an indirect cycle [29], and these systems are also smaller and simpler. Unfortunately, a steam turbine is not used for systems with VHTRs; this system was therefore rejected, and a gas propulsion solution was chosen instead (see Fig. 1).

For the propulsion system, a drive configuration could still be used by adjusting and implementing a gas turbine cycle. The literature describes two methods of power control for a closed Joule–Brayton cycle [30]:

- the use of a bypass valve in the low-temperature part of the cycle;
- the use of a gas extraction from the cycle to the tanks, i.e. a lower mass flow of the medium in the cycle.

The first method is less efficient than the second, but allows us to carry out a rapid load change. This approach has the further significant advantage of using less space in the engine room due to the absence of additional tanks for the storage of helium. The methods presented here change the amount of medium flowing through the turbine, while the pressure and temperature of the gas are constant. In addition, these solutions require only a small adjustment to the reactor reactivity, as the temperatures are constant and the power is controlled by the mass of the gas flowing through.

The gas cycle can be implemented in one of three configurations:

1. One turbine is connected to a compressor;
2. A separate compressor turbine and a power turbine are connected in series with it;
3. A separate compressor turbine and a power turbine are connected to it in parallel.

In solutions involving two turbines, a problem arises in that when a bypass is used, it creates a parallel arrangement. This layout means that the nominal gas flow must be supplied to the compressor turbine, so that in the case of a power turbine, enough medium must be provided to meet the needs of the propulsion system.

However, in all three cases, a positive impact of the proposed solution on the reduction of CO_2 emissions during the operation can be observed. For example, a ship with a nominal power (P_n) of 64 MW will emit at least aCO_2 = 21,120 kg of CO_2/h during its operation using a VHTR, as shown in Eq. (1). This is the least favourable result, as it is related to a propulsion system based on a gas–steam unit with emissivity gCO_2 = 330 kg/MWh, whereas with a VHTR, the emissive power is negligible. It is worth adding that the value of the parameter gCO_2 given here applies to modern power systems in which the thermodynamic parameters are at the highest levels [31], or where modern solutions based on a turbine and SOFC cell are introduced [32]. Due to the complexity of such solutions, it is difficult to maintain the compactness of the system, which is crucial on ships, and it is therefore reasonable to replace conventional fuel-based systems with VHTR cycles.

The solution presented here is also environmentally advantageous, and offers an opportunity to develop 'clean' ship propulsion. The reduction in CO_2 can be estimated as follows:

$$aCO_2 = P_n \cdot gCO_2, \tag{1}$$

where:

P_n – nominal power [MW]
gCO_2 – specific emission of CO_2 [kgCO_2/MWh]

EXTRACTION CONTROL OF THE THERMODYNAMIC CYCLE

Extraction control is used to adjust the power of a closed cycle by releasing some of the gas from the cycle into a tank. This gas is taken from the high-pressure, low-temperature part of the cycle (see Fig. 2), thus minimising the heat loss in the tank. The reduced mass of the medium causes a reduction in the mass flow rate, resulting in a lower power output. When it is necessary to increase the output, the working medium is supplied to the low-pressure, low-temperature parts of the cycle between the regenerative heat exchanger (RE) and the heat exchanger of the cooling system (COOL).

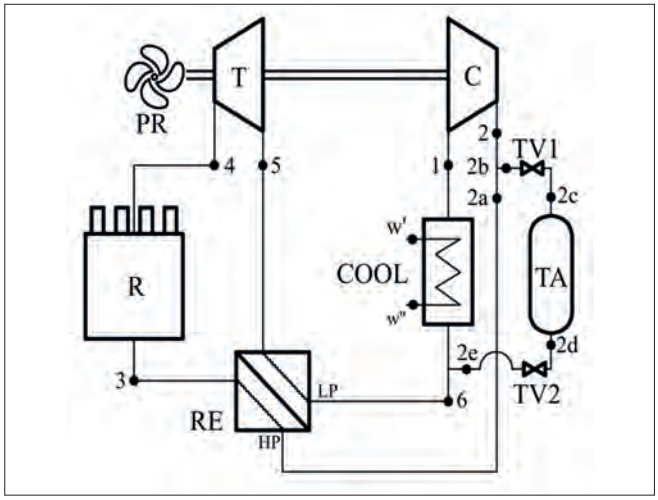

Fig. 2. Closed cycle with extraction control (TV – tank valve, TA – tank)

Using a smaller mass of the working medium allows for cycle operation at a constant temperature and pressure ratio, demonstrating that the turbine operates according to the intended thermodynamic cycle Fig. 1. This allows for constant values for the cycle efficiency and unit work. The local sound velocity remains unchanged by maintaining a constant temperature according to Eq. (2):

$$a = \sqrt{\frac{\kappa RT}{M}}, \tag{2}$$

where:

a – speed of sound [m/s]
κ – gas adiabatic exponent
T – absolute temperature [K]
R – molar gas constant [J/mol·K]
M – molar mass of gas [kg/mol]

The geometry of the vanes and flow channels gives constant Mach numbers [30], resulting in the same local flow speeds. At a constant flow speed, the value of the mass flow rate of the fluid is proportional to its density. The density for a constant temperature is also proportional to the absolute pressure. These relationships are true for an ideal gas, whereas in the case under consideration, the gaseous medium is helium; however, since it is an atomic gas, helium can be treated as a near-perfect gas. This form of control has one disadvantage in terms of the size of the helium tank, as 1 kg of helium occupies approximately 0.15 m^3 (at a pressure of 64.4 bar and a temperature of 170°C). The size of the tank here affects the control range, which is therefore limited.

BYPASS CONTROL FOR THE THERMODYNAMIC CYCLE

The second proposed solution is a bypass control, which involves releasing gas from the high-pressure part between the compressor (C) and the regenerative heat exchanger (RE) to the low-pressure region. The low-pressure part is located between the RE and the cooling system (COOL) (see Fig. 2). All of the medium in the cycle is compressed in the compressor C, and then some of this medium is throttled in a battery of bypass valves (or, in a simpler version, in a valve). This throttling process results in a decrease in the efficiency of the cycle. During the control process, there is almost no change in temperature, which is essential for durability reasons. Bypass control has the main advantage of reducing the space requirement for the gas tank, and a further benefit is that it enables rapid load change control with a 10% step change in output [30].

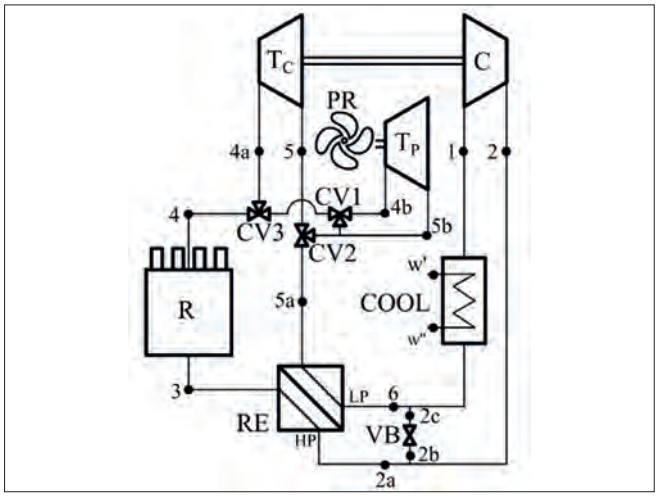

Fig. 3. Closed cycle with bypass control for two parallel turbine systems (T_C– compressor turbine, T_P– power turbine, VB – bypass valve, CV1–3 – control valves)

To determine the relationships resulting from the load-dependent change in cycle efficiency in Eq. (3)) this can be done by assuming the compressor's power and the turbine's effective power being changed. It can therefore be stated that:

$$\frac{\eta_p}{\eta_{100\%}} = \frac{N_p}{N_{e100\%}}, \tag{3}$$

where:

η_p – efficiency of the cycle at partial load
$\eta_{100\%}$ – efficiency of the cycle at full load
$N_{e\,p}$ – effective power at partial load
$N_{e\,100\%}$ – effective power at full load.

The efficiency can be calculated as shown in Eq. (4):

$$\eta = \frac{(l_T - l_C)}{q_R} = \frac{(i_4 - i_5) - (i_2 - i_1)}{(i_4 - i_3)} \tag{4}$$

where:

η – efficiency of the cycle
l_C – compressor unit work of the compressor, kJ/kg (value 1269 kJ/kg)
l_T – unit work of turbine, kJ/kg (value 588 kJ/kg)
q_R – difference in enthalpy values at the inlet and outlet (value 1381 kJ/kg)
i_1 – enthalpy value at point 1 (value 1708 kJ/kg)
i_2 – enthalpy value at point 2 (value 2296 kJ/kg)
i_3 – enthalpy value at point 3 (value 4967 kJ/kg)
i_4 – enthalpy value at point 4 (value 6348 kJ/kg)
i_5 – enthalpy value at point 5 (value 5079 kJ/kg)

The effective power at full load is used to estimate the mass flow rate of helium ($\dot{m}_{He}$) as shown in Eq. (5):

$$\dot{m}_{He} = \frac{N_{e100\%}}{(i_4 - i_5) - (i_2 - i_1)}. \tag{5}$$

The thermal power of the reactor ($\dot{Q}_R$ = 130 MW) can the be defined as given in Eq. (6):

$$\dot{Q}_R = \dot{m}_{He} \cdot q_R. \tag{6}$$

A theoretical comparison of the efficiency with the change in load for the different types of control discussed above is shown in Fig. 4.

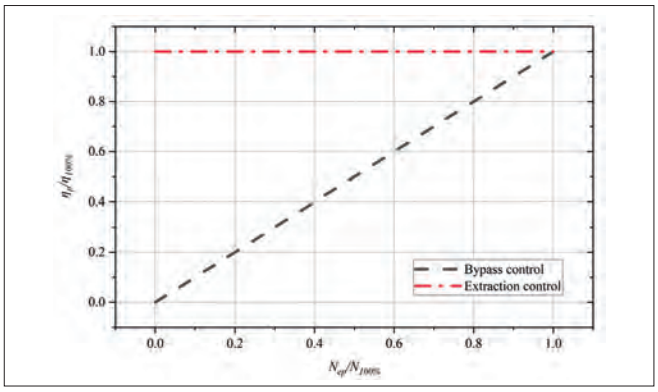

Fig. 4. Theoretical comparison of efficiency variation with change in load for different types of control

POSSIBLE CONFIGURATIONS OF THE TURBINE

In the systems mentioned above, the simplest configuration is obtained for a cycle with a single turbine to drive the compressor and the power receiver (propulsion). A more complicated cycle is obtained when there is a separate turbine for the compressor and the power receiver. In this approach, there are two individual turbines, which allows for increased cycle efficiency. In the case of a closed cycle, it is possible to design the system such that the turbine speed has an optimum value for the compressor and to plan the turbine power to meet the propulsion requirements.

Assumption for a single-turbine system

Examples of a system where a single turbine is used to drive the compressor and the power receiver on one shaft are shown in Figs. 1 and 2. The assumptions shown in Table 2 were made for a single turbine as a basic example, and cover all cases in respect to boundary conditions of the thermodynamic cycle. The mathematical model based on this assumption can easily be extended based on the phenomena described by Eqs. (10)–(18) to include other configurations and variations in the propeller power demand. When partial power is achieved, the turbine operates outside the contractual parameters. Moreover, the rotational speed of the compressor depends on the rotational speed required by the receiver. If the system only operates at partial power, then off-design operation takes place.

For the cycle shown in Fig. 1, calculations were carried out using the REFPROP and EkoPG programs, and the design values presented in Table 2 were assumed. Simplifications were introduced to indicate the capabilities of the system from a thermodynamic point of view, without taking into account the subsequent losses resulting from the transfer of propulsion to the propeller. An example of a system in which the thermodynamic parameters are considered is shown in Fig. 5. It is worth adding that in addition to thermodynamic analyses, data on mechanical losses, such as those resulting from friction in bearings or gears, can also be included in the EkoPG code, although these are not necessary for thermodynamic analysis.

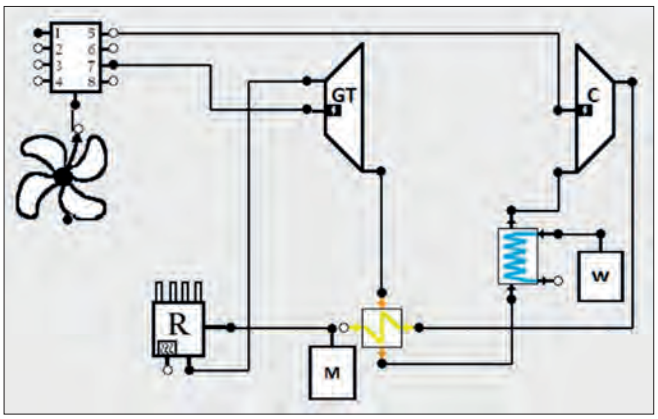

Fig. 5. System analysed in EkoPG software (GT – gas turbine, W – cooling water source, M – mass source of any mixture initiating the calculation)

The efficiency of the cycle (η) was obtained as 49% using Eq. (4). The mass flow rate for helium ($\dot{m}_{He}$) was also determined as 94 kg/s using Eq. (5); a knowledge of this quantity is necessary to estimate the size of the equipment needed for the cycle. Knowing $\dot{m}_{He}$ allows the thermal power of the reactor ($\dot{Q}_R$ = 130 MW) to be calculated using Eq. (6).

Given the thermal power of the reactor, it is possible to use the data presented for the VHTRs in Table 1 to estimate the dimensions of the THTR. The volume of the core (V_R = 21.7 m^3) for a core power density (φ_R) of 6 MW/m^3 can be calculated using Eq. (7) as follows:

$$V_R = \frac{\dot{Q}_R}{\varphi_R}. \tag{7}$$

If the reactor core is cylindrical, its dimensions can be estimated assuming a height-to-diameter ratio with an optimal value of approximately one [33]. This is due to the limitation on the possibility of helium pressure to drop when it flows through the reactor.

Tab. 2. Design values adopted for the thermodynamic analysis of the VHTR cycle in Fig. 1

Parameter	Symbol	Value	Units
Pressure of the medium at the reactor inlet	P_3	6.37	MPa
Temperature of the medium downstream of the reactor	T_4	1223	K
Ratio of expansion of turbines	Π_T	1.87	–
Pressure loss in the heat exchanger of the cooling system	Δp_R	140	kPa
Pressure loss in RE at the low-pressure side	Δp_{COOL}	50	kPa
Pressure loss in RE at the high-pressure side	Δp_{RE-LP}	50	kPa
Temperature difference at the low-temperature sides of RE	Δp_{RE-HP}	25	kPa
Temperature at the inlet to the compressor	ΔT_{RE-LP}	30	K
Efficiency of the regenerative heat exchanger	T_1	329	K
Efficiency of the compressor	δ_{RE}	0.96	–
Efficiency of the turbine	η_{iC}	0.915	–
Effective power of the turbine	η_{iT}	0.9	–
Effective power of the turbine	N_e	64,000	kW

The diameter of the core (D_R) can be determined by transforming the formula for the volume of a cylinder in Eq. (8), and is calculated as 3 m. The height of the core (H_R) is therefore also 3 m, as shown in Eq. (9).

$$D_R = \sqrt[3]{\frac{4 \cdot D_R}{\pi \cdot \frac{H_R}{D_R}}}, \tag{8}$$

$$H_R = \frac{D_R}{\frac{H_R}{D_R}}. \tag{9}$$

In addition to the dimensions given above, the thickness of a bio-shield of about 1 m must be taken into account, as well as other necessary components whose sizes are difficult to estimate, e.g. the fuel storage and feed system. However, if we compare these dimensions for the reactor with a typical slow-speed engine used on a 64 MW ship (e.g., the MAN 12G95ME,

which is over 23.7 m in length, 16 m in height, and 6.2 m in width), the dimensions of the reactor are much smaller. These calculations show that for the VHTR considered here, there is enough space in the engine room of a large container ship that it will be used to propel, thus avoiding the generation of CO_2.

System with two parallel turbines

Two turbines can be connected in parallel or in series, as mentioned previously. In this subsection, a system with a parallel connection [34] is considered, where a bypass control is used (cf. Fig. 3). The reason for this is that regardless of the level of drive load, the compressor has to compress all the medium that circulates in the cycle, which determines its nominal capacity. Operation of the compressor in the nominal work also means that the mass flow rate of the circulating medium is constant at the design level. A change in the mass flow rate is possible only in the turbine, due to the bypass valve. This leads to a difference in the turbine power, thus giving a change from a nominal to a partial load. This solution results in only the power turbine operating outside the design parameters.

As the power and compressor turbines are independent, they follow the same thermodynamic cycle [35], and therefore have the same inlet and outlet temperatures and expansion ratios. The only parameter that differentiates them is the mass flow rate of the working medium. Thus, it can be assumed that in this cycle, all the parameters at the characteristic points are the same as those for the cycle in question. These cycles also have the same efficiency under nominal power conditions. If it is assumed that there are no mechanical losses, the power of the compressor turbine is equal to the power of the compressor [36], and from this we can calculate the mass flow rate in the compressor turbine (T_C) using Eq. (10):

$$\dot{m}_{TC} = \frac{l_C}{l_T}\,\dot{m}_{He} = \frac{i_2 - i_1}{i_4 - i_5}\,\dot{m}_{He}\,. \tag{10}$$

The mass flow rate of the compressor turbine ($\dot{m}_{TC} = 43.6$ kg/s) is constant, and does not depend on the level at which the power turbine is loaded. Since the compressor turbine (T_C) operates here at full power, the mass flow rate occurring in the power turbine ($\dot{m}_{TP} = 50.4$ kg/s) can be calculated according to Eq. (11):

$$\dot{m}_{TP} = \dot{m}_{He} - \dot{m}_{TC}\,. \tag{11}$$

System with two turbines in series

The compressor turbine (T_C) and the power turbine (T_P) are connected in series (see Fig. 6), and operate according to different thermodynamic cycles since the medium entering the turbine is already partially expanded in the compressor turbine. This combination is used mainly for extraction control, where the amount of working medium in the cycle decreases under a partial load. The result is that the compressor (C) downloads less power, which varies approximately in proportion to the power generated by T_C. One advantage of this type of series system is that T_C can be designed with a speed of rotation according to the compressor demands. In this case, the speed of rotation for T_P is not dependent on the compressor and can be adjusted to the receiver's demand. Similarly, in the case of two turbines connected in parallel, the power of the compressor turbine (neglecting losses) must be equal to the power required by the compressor. However, since the mass flow rates are identical, their unit work must also be the same.

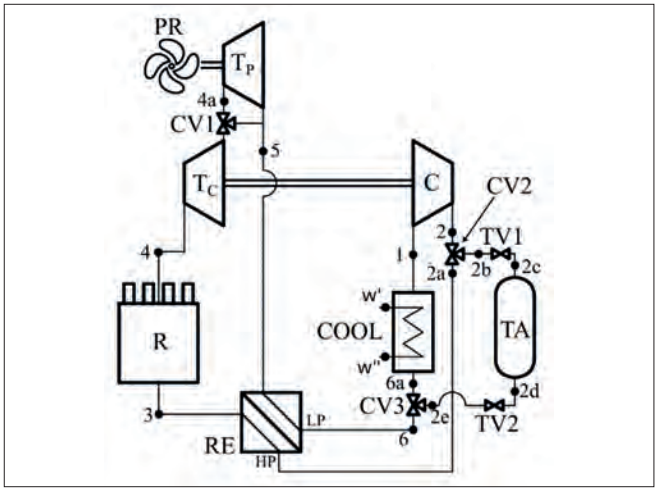

Fig. 6. Closed cycle with extraction control for two turbines in series

In view of the advantages and disadvantages described above, the cycle in Fig. 3 with bypass control and a split between the power and compressor turbines was chosen due to the limited space in the ship's power plant. For this system, the assumptions in Table 22 are appropriate, and these form the basis for further analysis.

METHODOLOGY OF ANALYSIS: THERMAL-FLOW CALCULATIONS UNDER VARYING OPERATING CONDITIONS

In this section of the paper, a thermal-flow methodology for the operation of a ship during a voyage with changing operating conditions will be presented.

ESTIMATION OF SEA WATER TEMPERATURE

It is assumed here that the only parameter of the helium that can change is the temperature. In addition, the pressure drops that occur in the heat exchangers depend on the relationship given in Eq. (12):

$$\Delta p = \Delta p(\dot{m}^2, d_h, A_C^2, L, \rho, f), \tag{12}$$

where:

Δp – pressure drop
$\dot{m}$ – mass flow rate
d_h – hydraulic diameter
A_C – total flow area of the medium on one side of the regenerative heat exchanger
L – length of the exchanger
ρ – density
f – friction coefficient

In this case, it has been stated that the dynamic viscosity of helium is constant. The variation in temperature in RE and COOL was determined by taking a constant temperature for both heat exchangers. The parameter shows the change in the temperature of the cooled or heated medium relative to the maximum difference in its temperature. The efficiency of the RE is assumed to be $\delta_{RE} = 0.96$ (see [37]), and that of the heat exchanger of the cooling system (COOL) is determined using the formula in Eq. (13):

$$\delta_{\mathrm{COOL}} = \frac{t_6 - t_1}{t_6 - t_{w'}}, \tag{13}$$

where

t_6 – temperature at point 6 point in Figure 5 (value 191°C)
t_1 – temperature at point 1 in Figure 5 (value 56°C)
$t_{w'}$ – water temperature [°C] in Figure 5 (value 80°C)

Once the efficiency value has been obtained, the temperature at point 1 can be calculated for the variable cooling water temperature using Eq. (14). At the same time, the temperature of the cooling water at the outlet uses the heat exchanged on both sides of the cooling system, as shown in Eq. (15):

$$t_1 = t_6 - \delta_{\mathrm{COOL}}(t_6 - t_{w'}), \tag{14}$$

$$t_{w''} = t_{w'} + \frac{\dot{m}_{He} C_{pHe}}{\dot{m}_w C_{pw}} (t_6 - t_1), \tag{15}$$

where:

$t_{w''}$ – temperature of the water at the cooling system outlet
C_{pHe} – average specific heat capacity of helium, $C_{pHe} = 5.19$ kJ/kgK
C_{pw} – average specific heat capacity of water, $C_{pw} = 4.19$ kJ/kgK

A change in temperature at the compressor inlet results in a change in temperature at the compressor outlet, while the temperature at point 3 is calculated based on the assumed temperature efficiency of the RE (see Fig. 3). The helium in the VHTR is heated to a constant temperature, resulting in no temperature change at the turbine outlet. These variations in temperature occurring at the RE outlet (see Fig. 7) are taken into consideration in the cooling system calculations as follows:

$$t_6 = t_5 - \frac{\dot{m}_{He} C_{pHe}}{\dot{m}_{He} C_{pHe}} (t_3 - t_2). \tag{16}$$

The helium at the inlet has a temperature higher than that of sea water, meaning that an iterative calculation is required for each seawater value, and a program for this was created based on the block diagram in Fig. 7.

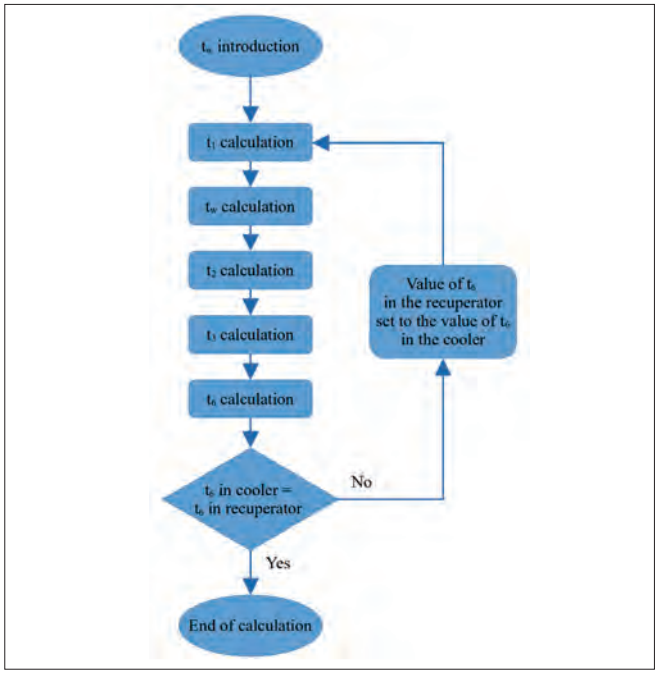

Fig. 7. Block diagram used to create the numerical program to calculate the thermal cycle temperatures under consideration

ESTIMATION OF VARIATION IN PROPELLER POWER DEMAND

As mentioned earlier, a cycle with bypass control and a split between a power turbine and a compressor turbine was chosen for consideration (Fig. 3). During the voyage of the ship, the power demand varies from zero, when the ship is stationary, to a transient maximum value that occurs during the journey. It is assumed that the compressor turbine operates at its maximum power at all times (with a constant mass flow rate) and only the power for the power turbine varies (i.e., the mass flow rate to RE is variable). Hence, in the flow through the regenerative heat exchanger, there are changes in the pressure and flow rate, resulting in adjustments to the pressure drops and heat transfer efficiency. These values are considered to be negligible in the overall cycle. The design of the plate-fin exchanger allows the helium mass flow rate to be split such that the flow is constant in specific channels of the exchanger. The variable pressure resulting from the varying mass flow in the fixed channels has also been determined. The assumptions in Eq. (17) are also made:

$$\begin{aligned} l_t &= const, \\ q_R &= const. \end{aligned} \tag{17}$$

In this case, the combination of the helium mass flow rate flowing through the bypass with the mass flow rate leaving the RE should also be considered. Since the specific enthalpies of helium are almost identical in the cycles at points 2 and 6 (this differs by 5%), this factor can be neglected. The helium pressure is reduced by isenthalpic throttling in the bypass valves to the pressure level prevailing downstream of the RE.

As a simplification, we treat the values of the helium-specific enthalpy found at these points as the same as the calculated values for the nominal output. The efficiency of the cycle can be written as shown below:

$$\eta = \frac{N_{TP}}{\dot{Q}_R} = \frac{\dot{m}_{TP} \cdot l_t}{q_R \cdot (\dot{m}_{TP} + \dot{m}_{TC})} = \frac{l_t}{q_R} \cdot \frac{\dot{m}_{TP}}{\dot{m}_{TP} + \dot{m}_{TC}}, \quad (18)$$

where:
NTP – propeller turbine power

RESULTS AND DISCUSSION

In this section, the results of calculations for the operation of a ship during a voyage with changing operating conditions will be presented and discussed. The values obtained for the system in the nominal case (i.e. without changing operating conditions) have been given in the section entitled "Proposed propulsion system with VHTR for a container ship". These calculations form the basis for the design of the gas cycle. In a real system, there are changes in the operation of the whole system, but in this case, our focus was only on the efficiency of the cycle, i.e. the variation in sea water temperature and propeller demand power.

SEA WATER TEMPERATURE

The bodies of water found throughout the world and used for cooling have different temperatures. In our case, water is used in the closed-gas cycle to cool the helium upstream of the compressor. The temperature of the compressed medium affects the work required to compress it to the correct pressure level, meaning that the cooling water taken from the sea or ocean changes the efficiency of the entire cycle. It is assumed here that the ship is cruising in either Arctic or tropical waters; in other words, the temperature range is between 2°C and 32°C. Once the temperatures had been determined, the cycle was recalculated, producing the results presented in Figs. 8, 9 and10.

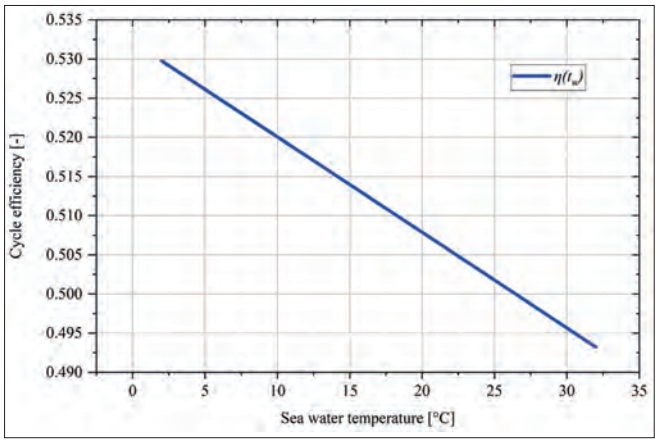

Fig. 8. Relationship between cycle efficiency and sea water temperature

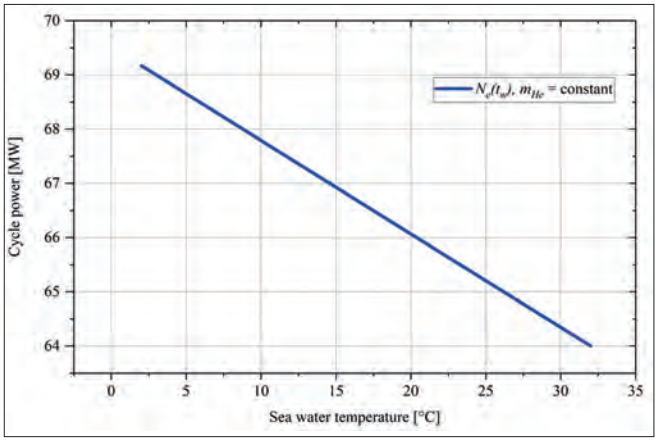

Fig. 9. Relationship between cycle power output and seawater temperature at a constant mass flow rate of helium

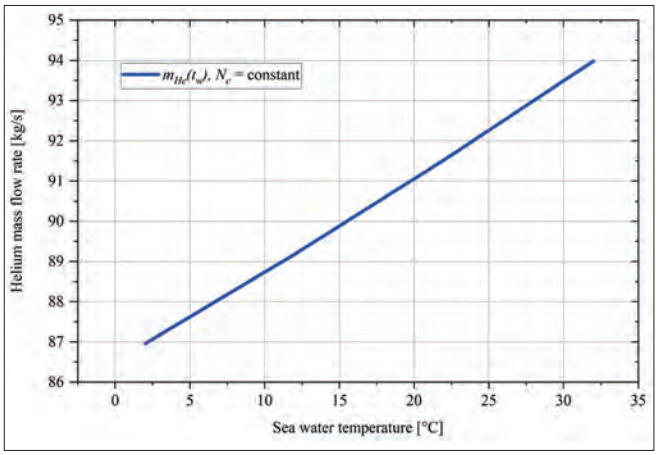

Fig. 10 Relationship between helium mass flow rate and sea water temperature at constant power output

Once the calculations presented here have been performed, it can be concluded that the efficiency of the cycle is higher when the temperature of the seawater is lower. However, this leads to an increase in the power generated by the turbine, which can be dangerous in terms of overloading. It is therefore necessary, despite the use of bypass control, to carry out additional extraction of the medium from the cycle. In the seawater temperature range considered here, up to 8% of the helium mass flow rate should be released to keep the shaft power constant.

Due to the use of the VHTR at low temperatures, it is important to use a gas tank, and more specifically, a helium tank. This tank must have sufficient volume to store excess helium when the ship travels through bodies of water with low temperatures.

The situation is different when there is limited power on the shaft. The control method proposed here means that the reactor need not extinguished even when the ship is stationary in the harbour, although this leads to the continuous burning of nuclear fuel and operation at zero efficiency.

VARIATION IN PROPELLER ENGINE POWER DEMAND

As the power of the power turbine ($N_{e100\%}$) is directly proportional to the mass flow rate of helium, as shown in Eq. (5), we can say that the efficiency of the cycle is a measurable function of the power supplied to the propeller (Fig. 11). In contrast, the reactor power is linearly dependent on the power demanded by the propeller, and its minimum value when operating only the compressor turbine is approximately 45% (Fig. 12).

During a voyage, on the other hand, the thermal energy rate of the reactor should be limited to the power required by the propeller. The lower the load, the lower the overall cycle efficiency. However, this is not a linear relationship: for example, 40% and 20% reductions in power lead to decreases in efficiency of only approximately 20% and 10%, respectively. Thus, it can be assumed that these decreases are accepTable 2for regular operation at close to nominal power. Based on these findings, we suggest that nuclear propulsion could play a vital role in the future of ship technology, although further research is required to fully understand its potential and limitations.

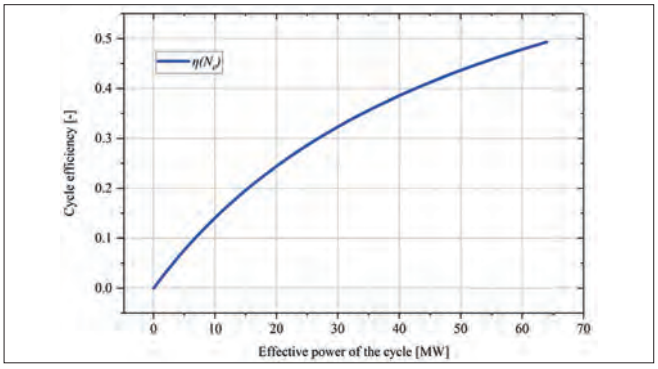

Fig. 11. Relationship between cycle efficiency and power required by the propeller with bypass control

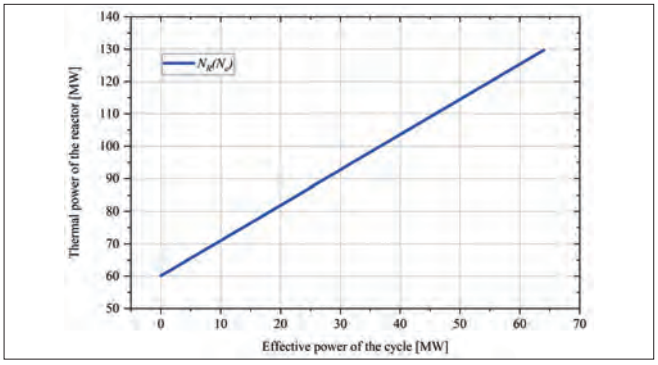

Fig. 12. Relationship between reactor thermal power requirements and propeller power requirements

COMPARISON WITH THE SELECTED VHTRS AND SAFETY ISSUES

Nuclear ship propulsion is currently used in military ships and icebreakers [38]. Examples of other nuclear-powered ships include *Otto Hahn*, *NS Savannah*, *Mutsu*, and *NS Sevmorput* [39,40]. The use of reactors on passenger or cargo ships raises concerns about the safety of those on board, and new nuclear reactors therefore have additional safety features for use on these ships. Such energy sources are fourth-generation reactors that are characterised by increased operational safety and reliability, and are less expensive than older reactors [41]. To increase security, gas-cooled reactors should be considered [42]. An additional advantage of nuclear propulsion is the lower fuel cost compared to traditional fuels; it can also be used in ships that have already been built if these are modernised, as we have demonstrated in a previous paper [19].

The focus of this article is on the VHTR, which belongs to the fourth generation of these devices [43,44] and is the successor to the HTGR [45]. It has a high degree of safety [46] based on the elimination of severe accidents, which is very important when installed on ships. In terms of financial considerations, they have the great advantage of efficient use of nuclear fuel for energy production, resulting in fewer purchase expenditures. A VHTR is cooled by helium gas, which is chemically inactive, and, more importantly for use in floating facilities, is non-toxic and non-flammable [47,48]. This process is characterised by high efficiency, which is achieved using a high-temperature gas turbine (900°C and 8.5 MPa). The operating research equipment's are presented in Table 3 according to [33,49]. The HTTR, GTHTR300, and THTR devices shown here can be classified as VHTRs, whereas the HTR-10 can be classified as an HTR (owing to the lower coolant temperature at the reactor outlet). It is mentioned here as an example of the use of an indirect cycle.

In Table 3, the proposed system in the article is related to the quantitative parameter which is thermal power of reactor. The assumed value is within the range of the other powers and this confirms the validity of the feasibility of such a solution on ships. Also the qualitative thermodynamic parameters of the proposed system are comparable to the literature data [33,49]. To be determined is the 'Type of reactor core', but this is a future work that the authors have not undertaken in this article However, it should be noted that this system has been introduced to a container ship, which represents a significant novel aspect of this article.

Tab. 3. Comparison of selected VHTRs [33,49]

	HTTR	HTR-10	GTHTR 300	THTR	Proposed system
Thermal power [MW]	30	10	600	750	130
Temperature of coolant at inlet [°C]	950	700	950	850	950
Pressure of coolant [MPa]	4	3	6.4	4	6.37
Power density of core [MW/m^3]	2.5	2	5.4	6	6
Type of cycle	Direct	Indirect	Direct	Direct	Direct
Type of reactor core	Prismatic	Pebble bed	Prismatic	Pebble bed	Will be selected in future

A VHTR may use a direct cycle with a gas turbine or an indirect cycle with a steam or gas turbine. A direct cycle has the advantage of being simple in design, which increases the reliability of the facility, and is most commonly used because it enables high efficiency to be achieved using high temperatures. However, this approach also has the disadvantage of undesirable contamination of the non-nuclear part by radionuclides transported with helium [50]. In the case of a direct cycle, a limitation arises from the helium flowing through the reactor and its confinement behind the bioshell. The problem resulting from the radioactivity of the helium supplied directly to the gas turbine is solved by installing a purification system to remove undesirable elements from the helium. Furthermore, a direct cycle is more efficient than an indirect one, since the medium flow at the turbine inlet has a higher temperature, and an indirect cycle has a more complex design, due to the need for more components [30].

SUMMARY

The main motivation for this work arose from the pressing need to reduce greenhouse gas emissions in the maritime industry in accordance with international environmental regulations. To meet this requirement, the possibility of using a VHTR on a ship was proposed. Taking into consideration the power of nuclear reactors, this system was adapted to a large container ship. The thermodynamic efficiency of the VHTR system was comprehensively investigated under various operating conditions when cruising in different bodies of water, with different seawater temperatures and propulsion power requirements.

We have described a VHTR reactor with extremely high thermal stability; as a result, the risk of accidents resulting from the reactor overheating is significantly reduced compared to other types of nuclear reactor. An important feature of the reactors discussed in this paper is that passive safety systems are particularly important on ships where people are constantly present, meaning that additional protection needs to be provided. Furthermore, VHTR reactors are highly resistant to mechanical shocks, which is essential given the possibilities for harsh weather and wave action during a voyage.

To date, VHTR reactors have not been used or tested on ships. The characteristics of these reactors and the thermodynamic cycle that was designed here to operate with them were based on descriptions in the literature of land-based applications of VHTR technology, mainly in test power plants.

VHTRs are fuelled by TRISO fuels, which offer an additional layer of protection against the release of radioactive materials in the event of an accident. The high thermal efficiency of these reactors, which reaches 45–50%, translates to significantly lower fuel consumption compared to traditional ship fuel. This, in turn, reduces greenhouse gas emissions, which is essential to meet international environmental requirements, especially the "Fit for 55" regulations. For shipowners, the use of low-emission technologies is advantageous, as it enables them to obtain environmental certification and tax credits, which contribute to further savings and increased competitiveness in the transportation market.

Although the initial costs associated with adapting ships to VHTRs may be higher than for conventional propulsion, such reactors can generate significant savings in the long term through lower fuel costs and reduced maintenance requirements. With longer refuelling intervals, ships can operate more efficiently and autonomously, leading to increased profits for shipowners by reducing logistics costs and decreasing the frequency of technical inspections and maintenance.

It should also be noted that the higher efficiency of thermodynamic cycles with VHTR reactors means that more of the energy produced is used to propel the vessel and less is lost as heat, further contributing to fuel savings and reduced operating costs. The cost of nuclear fuel is also more predictable, as its price remains relatively constant, unlike fossil fuels, whose prices are prone to large fluctuations in global markets, making long-term financial planning difficult.

In summary, the use of VHTR reactors on ships could provide significant economic benefits through fuel savings, increased payload capacity, or, most importantly, compliance with environmental regulations that aim for zero-carbon ships. With planning and new investments, VHTR-powered ships can revolutionise maritime transportation by providing a sustainable and economically viable alternative to traditional fuels for shipping. This article represents a key step towards achieving sustainable maritime transport regulations and meeting stringent international environmental standards.

ACKNOWLEDGEMENTS

Financial support for these studies from Gdańsk University of Technology via grant DEC–50/2020/IDUB/I.3.3 under the ARGENTUM TRIGGERING RESEARCH GRANTS – EIRU program is gratefully acknowledged. This research was supported by CI TASK (Poland).

REFERENCES

1. Ertesvåg IS, Madejski P, Ziółkowski P, Mikielewicz D. Exergy analysis of a negative CO2 emission gas power plant based on water oxy-combustion of syngas from sewage sludge gasification and CCS. Energy 2023, 278:127690. https://doi.org/10.1016/j.energy.2023.127690.

2. Bąk K, Ziółkowski P, Frost J, Drosińska-Komor M. Comparative study of a combined heat and power plant retrofitted by CO2 capture during the combustion of syngas from sewage sludge gasification versus zero-emission combustion of hydrogen produced using renewables. Int J Hydrogen Energy 2023, 48:39625–40. https://doi.org/10.1016/j.ijhydene.2023.07.322.

3. Ziółkowski P, Szewczuk-Krypa N, Butterweck A, Stajnke M, Głuch S, Drosińska-Komor M, et al. Comprehensive thermodynamic analysis of steam storage in a steam cycle in a different regime of work: A zero-dimensional and

three-dimensional approach. J Energy Resour Technol 2021, 143:1–27. https://doi.org/10.1115/1.4052249.

4. Papadis E, Tsatsaronis G. Challenges in the decarbonization of the energy sector. Energy 2020, 205:118025. https://doi.org/10.1016/j.energy.2020.118025.

5. Baste IA, Watson RT. Tackling the climate, biodiversity and pollution emergencies by making peace with nature 50 years after the Stockholm Conference. Glob Environ Chang 2022, 73:102466. https://doi.org/10.1016/j.gloenvcha.2022.102466.

6. Montoro-Ramírez EM, Parra-Anguita L, Álvarez-Nieto C, Parra G, López-Medina I. Effects of climate change in the elderly's health: a scoping review protocol. BMJ Open 2022, 12:e058063. https://doi.org/10.1136/bmjopen-2021-058063.

7. Cifuentes-Faura J. European Union policies and their role in combating climate change over the years. Air Qual Atmos Heal 2022, 15:1333–40. https://doi.org/10.1007/s11869-022-01156-5.

8. Cloete S, Ruhnau O, Hirth L. ScienceDirect On capital utilization in the hydrogen economy : The quest to minimize idle capacity in renewables- rich energy systems. Int J Hydrogen Energy 2020, 46:169–88. https://doi.org/10.1016/j.ijhydene.2020.09.197.

9. Cownden R, Mullen D, Lucquiaud M. Towards net-zero compatible hydrogen from steam reformation – Techno-economic analysis of process design options. Int J Hydrogen Energy 2023, 48:14591–607. https://doi.org/10.1016/j.ijhydene.2022.12.349.

10. Szturgulewski K, Głuch J, Drosińska-Komor M, Ziółkowski P, Gardzilewicz A, Brzezińska-Gołębiewska K. Hybrid geothermal-fossil power cycle analysis in a Polish setting with a focus on off-design performance and CO2 emissions reductions. Energy 2024, 299:131382. https://doi.org/10.1016/j.energy.2024.131382.

11. Olszewski W, Dzida M, Nguyen VG, Cao DN. Reduction of CO 2 Emissions from Offshore Combined Cycle Diesel Engine-Steam Turbine Power Plant Powered by Alternative Fuels. Polish Marit Res 2023, 30:71–80. https://doi.org/10.2478/pomr-2023-0040.

12. Duwe M, Graichen J, Böttcher H. Can current EU climate policy reliably achieve climate neutrality by 2050? 2023.

13. No Title n.d. https://climate.ec.europa.eu/eu-action/transport-emissions/reducing-emissions-shipping-sector_pl (accessed 20 August 2023).

14. Sumin M. Challenges of implementing sustainable solutions in commercial shipping. Arcada University of Applied Sciences: International Business, 2023.

15. Deng W, Zhang X, Zhou Y, Liu Y, Zhou X, Chen H, et al. An enhanced fast non-dominated solution sorting genetic algorithm for multi-objective problems. Inf Sci (Ny) 2022, 585:441–53. https://doi.org/10.1016/j.ins.2021.11.052.

16. Bäckstrand K. Towards a Climate-Neutral Union by 2050? The European Green Deal, Climate Law, and Green Recovery. Routes to a Resilient Eur. Union, Cham: Springer International Publishing; 2022, p. 39–61. https://doi.org/10.1007/978-3-030-93165-0_3.

17. Szewczuk-Krypa N, Grzymkowska A, Głuch J. Comparative Analysis of Thermodynamic Cycles of Selected Nuclear Ship Power Plants with High-Temperature Helium-Cooled Nuclear Reactor. Polish Marit Res 2018, 25:218–24. https://doi.org/10.2478/pomr-2018-0045.

18. Szewczuk-Krypa N, Drosińska-Komor M, Głuch J, Breńkacz Ł. Comparison Analysis of Selected Nuclear Power Plants Supplied with Helium from High-Temperature Gas-Cooled Reactor. Polish Marit Res 2018, 25:204–10. https://doi.org/10.2478/pomr-2018-0043.

19. Drosińska-Komor M, Głuch J, Breńkacz Ł, Ziółkowski P. On the Use of Selected 4th Generation Nuclear Reactors in Marine Power Plants. Polish Marit Res 2022, 29:76–84. https://doi.org/10.2478/pomr-2022-0008.

20. Significant Ships of 2018, The Royal Institution of Naval Architects, 2019. n.d.

21. Significant Ships of 2019, The Royal Institution of Naval Architects, 2020. n.d.

22. Significant Ships of 2020, The Royal Institution of Naval Architects, 2021. n.d.

23. Gutowska I, Woods BG, Cadell SR. CFD modeling of the OSU High Temperature Test Facility inlet plenum flow distribution during normal operation. Nucl Eng Des 2019, 353:110216. https://doi.org/10.1016/j.nucengdes.2019.110216.

24. Kadak AC. The Status of the US High-Temperature Gas Reactors. Engineering 2016, 2:119–23. https://doi.org/10.1016/J.ENG.2016.01.026.

25. Forsberg CW. Roadmap of Graphite Moderator and Graphite-Matrix TRISO Fuel Management Options. Nucl Technol 2024, 210:1623–38. https://doi.org/10.1080/00295450.2024.2337311.

26. Trela M, Kwidziński R, Głuch J, Butrymowicz D. Analysis of application of feed-water injector heaters to steam power plants. Polish Marit Res 2009, 16:64–70. https://doi.org/10.2478/v10012-008-0047-z.

27. Alzayedi AMT, Batra A, Sampath S, Pilidis P. Techno-Environmental Mission Evaluation of Combined Cycle Gas

Turbines for Large Container Ship Propulsion. Energies 2022, 15:4426. https://doi.org/10.3390/en15124426.

28. Niksa-Rynkiewicz T, Witkowska A, Głuch J, Adamowicz M. Monitoring the Gas Turbine Start-Up Phase on a Platform Using a Hierarchical Model Based on Multi-Layer Perceptron Networks. Polish Marit Res 2022, 29:123–31. https://doi.org/10.2478/pomr-2022-0050.

29. Błaszczyk A, Głuch J, Gardzilewicz A. Operating and economic conditions of cooling water control for marine steam turbine condensers. Polish Marit Res 2011, 18:48–54. https://doi.org/10.2478/v10012-011-0017-8.

30. Dostal V, Driscoll M., Hejzlar P. A supercritical carbon dioxide cycle for next generation nuclear reactors, MIT-ANP-TR-100, advanced nuclear power technology program report. Cambridge (MA): Massachusetts Institute of Technology. 2004.

31. Kotowicz J, Brzęczek M, Job M. The thermodynamic and economic characteristics of the modern combined cycle power plant with gas turbine steam cooling. Energy 2018, 164:359–76. https://doi.org/10.1016/j.energy.2018.08.076.

32. Badur J, Lemański M, Kowalczyk T, Ziółkowski P, Kornet S. Zero-dimensional robust model of an SOFC with internal reforming for hybrid energy cycles. Energy 2018, 158:128–38. https://doi.org/10.1016/j.energy.2018.05.203.

33. Kugeler, K., Nabielek H, Buckthorpe D. The High Temperature Gas-cooled Reactor: Safety considerations of the (V)HTR-Modul. European Atomic Energy Community; 2017. https://doi.org/10.2760/270321.

34. Głuch J, Krzyżanowski J. New attempt for diagnostics of the geometry deterioration of the power system based on thermal measurement. Proc. ASME Turbo Expo 2006, vol. 2, Barcelona: 2006, p. 531–9.

35. Głuch J. Selected problems of determining an efficient operation standard in contemporary heat-and-flow diagnostics. Polish Marit Res 2009, 16:22–6. https://doi.org/10.2478/v10012-008-0040-6.

36. Breńkacz Ł. Bearing Dynamic Coefficients in Rotordynamics: Computation Methods and Practical Applications (Wiley-ASME Press Series). 2021.

37. Sato H, Yan XL, Tachibana Y, Kunitomi K. GTHTR300 – A nuclear power plant design with 50% generating efficiency. Nucl Eng Des 2014, 275:190–6. https://doi.org/10.1016/j.nucengdes.2014.05.004.

38. Freire LO, De Andrade DA. Historic survey on nuclear merchant ships. Nucl Eng Des 2015, 293:176–86. https://doi.org/10.1016/j.nucengdes.2015.07.031.

39. Islam Rony Z, Mofijur M, Hasan MM, Rasul MG, Jahirul MI, Forruque Ahmed S, et al. Alternative fuels to reduce greenhouse gas emissions from marine transport and promote UN sustainable development goals. Fuel 2023, 338:127220. https://doi.org/10.1016/j.fuel.2022.127220.

40. Alam SB, de Oliveira RGG, Goodwin CS, Parks GT. Coupled neutronic/thermal-hydraulic hot channel analysis of high power density civil marine SMR cores. Ann Nucl Energy 2019, 127:400–11. https://doi.org/10.1016/j.anucene.2018.12.031.

41. Freitas Neto LG de, Freire LO, Dos Santos A, De Andrade DA. Potential advantages of molten salt reactor for merchant ship propulsion. Brazilian J Radiat Sci 2021, 9:1–18. https://doi.org/10.15392/bjrs.v9i2b.1466.

42. Garcia RF, Carril JC, Catoira AD, Gomez JR. Efficiency enhancement of GT-MHRs applied on ship propulsion plants. Nucl Eng Des 2012, 250:326–33. https://doi.org/10.1016/j.nucengdes.2012.06.013.

43. Kim ES, Oh CH, Sherman S. Simplified optimum sizing and cost analysis for compact heat exchanger in VHTR. Nucl Eng Des 2008, 238:2635–47. https://doi.org/10.1016/j.nucengdes.2008.05.012.

44. Gutowska I, Woods BG, Halsted J. Developing PCC and DCC integral effects test experiments at the High Temperature Test Facility. Front Energy Res 2023, 11:1–15. https://doi.org/10.3389/fenrg.2023.1088070.

45. Kowalczyk T, Głuch J, Ziółkowski P. Analysis of Possible Application of High-Temperature Nuclear Reactors to Contemporary Large-Output Steam Power Plants on Ships. Polish Marit Res 2016, 23:32–41. https://doi.org/10.1515/pomr-2016-0018.

46. Park MY, Kim ES. Thermodynamic evaluation on the integrated system of VHTR and forward osmosis desalination process. Desalination 2014, 337:117–26. https://doi.org/10.1016/j.desal.2013.11.023.

47. Ueta S, Aihara J, Sawa K, Yasuda A, Honda M, Furihata N. Development of high temperature gas-cooled reactor (HTGR) fuel in Japan. Prog Nucl Energy 2011, 53:788–93. https://doi.org/10.1016/j.pnucene.2011.05.005.

48. Locatelli G, Mancini M, Todeschini N. Generation IV nuclear reactors: Current status and future prospects. Energy Policy 2013, 61:1503–20. https://doi.org/10.1016/j.enpol.2013.06.101.

49. Yan XL. Very high-temperature reactor. In: Pioro IL, editor. Handb. Gener. IV Nucl. React. Woodhead P, Elsevier; 2016, p. 55–90. https://doi.org/10.1016/B978-0-08-100149-3.00003-3.

50. Klisińska M. Wysokotemperaturowe Reaktory VHTR – Geneza, Badania, Status. Perspektywy Zastosowania. vol. 2008. n.d.